

# PROCEEDINGS OF SPIE

[SPIDigitalLibrary.org/conference-proceedings-of-spie](https://spiedigitallibrary.org/conference-proceedings-of-spie)

## Dynamical graph theory networks techniques for the analysis of sparse connectivity networks in dementia

Tahmassebi, Amirhessam, Pinker-Domenig, Katja, Wengert, Georg, Lobbes, Marc, Stadlbauer, Andreas, et al.

Amirhessam Tahmassebi, Katja Pinker-Domenig, Georg Wengert, Marc Lobbes, Andreas Stadlbauer, Francisco J. Romero, Diego P. Morales, Encarnacion Castillo, Antonio Garcia, Guillermo Botella, Anke Meyer-Bäse, "Dynamical graph theory networks techniques for the analysis of sparse connectivity networks in dementia," Proc. SPIE 10216, Smart Biomedical and Physiological Sensor Technology XIV, 1021609 (16 May 2017); doi: 10.1117/12.2263555

**SPIE.**

Event: SPIE Commercial + Scientific Sensing and Imaging, 2017, Anaheim, California, United States

# Dynamical Graph Theory Networks Techniques for the Analysis of Sparse Connectivity Networks in Dementia

Amirhessam Tahmassebi<sup>a</sup>, Katja Pinker-Domenig<sup>a,b,c</sup>, Georg Wengert<sup>b</sup>, Marc Lobbes<sup>d</sup>,  
Andreas Stadlbauer<sup>e</sup>, Francisco J. Romero<sup>f</sup>, Diego P. Morales<sup>f</sup>, Encarnacion Castillo<sup>f</sup>,  
Antonio Garcia<sup>f</sup>, Guillermo Botella<sup>g</sup>, and Anke Meyer-Bäse<sup>a</sup>

<sup>a</sup> Department of Scientific Computing,  
Florida State University, Tallahassee, Florida 32310-4120, USA

<sup>b</sup> Medical University of Vienna, Vienna, Austria

<sup>c</sup> Memorial Sloan-Kettering Cancer Center, New York, USA

<sup>d</sup> Department of Radiology and Nuclear Medicine, Maastricht University Medical Center,  
Maastricht, The Netherlands

<sup>e</sup> Department of Neurosurgery, University of Erlangen-Nürnberg, Germany

<sup>f</sup> Department of Electronics and Computer Technologies, Facultad de Ciencias, Granada, Spain

<sup>g</sup> Department of Computer Architecture, Universidad Complutense de Madrid, Madrid, Spain

## ABSTRACT

Graph network models in dementia have become an important computational technique in neuroscience to study fundamental organizational principles of brain structure and function of neurodegenerative diseases such as dementia. The graph connectivity is reflected in the connectome, the complete set of structural and functional connections of the graph network, which is mostly based on simple Pearson correlation links.

In contrast to simple Pearson correlation networks, the partial correlations (PC) only identify direct correlations while indirect associations are eliminated. In addition to this, the state-of-the-art techniques in brain research are based on static graph theory, which is unable to capture the dynamic behavior of the brain connectivity, as it alters with disease evolution. We propose a new research avenue in neuroimaging connectomics based on combining dynamic graph network theory and modeling strategies at different time scales. We present the theoretical framework for area aggregation and time-scale modeling in brain networks as they pertain to disease evolution in dementia. This novel paradigm is extremely powerful, since we can derive both static parameters pertaining to node and area parameters, as well as dynamic parameters, such as system's eigenvalues. By implementing and analyzing dynamically both disease driven PC-networks and regular concentration networks, we reveal differences in the structure of these network that play an important role in the temporal evolution of this disease. The described research is key to advance biomedical research on novel disease prediction trajectories and dementia therapies.

**Keywords:** Graph theory, nonlinear dynamics, dynamic graph, clustering, correlation, dementia

## 1. INTRODUCTION

Novel mathematical concepts such as graph theoretical techniques can capture the brain connectivity and its topology.<sup>FZPB12, GT12, ZSL<sup>+</sup>12</sup> These graph networks are mostly based on Pearson correlation and are capturing either the structural and/or functional brain connectivity. From these graphs, new descriptors can be derived to quantify induced changes in topology or network organization, or serve as theory-driven biomarkers to predict dementia at the level of the individual subject.

While most graph networks applied to dementia research, even for longitudinal data are static graph networks, which cannot capture the dynamical processes governing the time evolution of dementia. Therefore, a new paradigm in dementia research - dynamical graph networks - is required to advance this field and overcome the obstacles posed by static graph theory in terms of disease prediction, evolution, and its associated connectivity changes.

Smart Biomedical and Physiological Sensor Technology XIV, edited by  
Brian M. Cullum, Douglas Kiehl, Eric S. McLamore, Proc. of SPIE Vol. 10216,  
1021609 · © 2017 SPIE · CCC code: 0277-786X/17/\$18 · doi: 10.1117/12.2263555

To address this important issue of analyzing the dynamical behavior, we propose a simplified method resulting in a model of lower complexity. Balanced truncation is known as the standard method for model reduction.<sup>Moo81</sup> It is based on a state-space point of view of employing the well-known observability and controllability Gramians<sup>MBTC11, LMG02, Sch93</sup> and related to the past input energy (controllability) and future input energy (observability). While for linear systems this procedure is pretty straightforward, for nonlinear systems balancing truncation becomes in general not a simple task.<sup>MB08, MBT08a</sup> However they are not quite efficient in terms of model reduction for large-scale networks. For brain connectivity models, we require a structure preservation between subsystems and at the same time, a network topology-preserving mechanism to provide model reduction. We will address this issue by choosing a technique based on an area aggregation and time-scale modeling for sparse brain networks with densely interconnected hubs and externally sparse interconnections between these hubs. In<sup>CK85</sup> was shown that the neurons in the hubs synchronize on the fast time-scale and as aggregated neurons determine the slow dynamics of the neural network. We apply our novel concepts on connectivity networks from.<sup>WJM<sup>+</sup>12</sup> There was the morphometry-based connection concept with cortical gray matter thickness has been applied. 645 automatically parcellated cortical volumes were derived to study the underlying architecture of the brain network. The connectivity matrices from the concentration method of calculating a partial correlation (PC) and a modified version of the PC algorithm, the so-called P\*<sup>WJM<sup>+</sup>12</sup> were analyzed in terms of a reduced-model approximation over time for the left and right hemisphere. Gray matter thickness is known to play an important role in Alzheimer's disease,

## 2. REDUCED-MODEL APPROXIMATION OVER TIME

The idea of two-time scale systems has been widely studied in connections with dynamical systems.<sup>SK84, MBRT10, MBRY07, MBKI</sup>

Graph networks that exhibit a structure of dense clustered areas but have sparse connections between these areas can be dynamically approximated by a two-time scale system, where the neurons within the same area synchronize on the fast time-scale, because the dense within-area connections drive the nodes of the given area quickly to reach an equilibrium.

At the same time, the exchange between the areas is based on sparse connections and can be described at a slow time-scale. This coupled dynamics leads to a reduced-order model describing the long-term behavior of the overall network. The large-scale brain network is viewed as an interconnected graph with links between the areas which are viewed as nodes in the graph. Two main parameters are describing such a network:<sup>CK85</sup> the node parameter  $d$  and the area parameter  $\delta$ . The node parameter is given as:

$$d = \frac{c^E}{c^I} \ll 1 \quad (1)$$

where  $c^E$  are the densest external links over all nodes and areas and  $c^I$  are sparsest internal links over all existing areas.  $d$  needs to be a small number. The area parameter is given as

$$\delta = \frac{\gamma^E}{mc^I} \ll 1 \quad (2)$$

where  $\gamma^E$  are the densest external links over all areas and  $m$  is the minimal number of nodes found in an area.

In order to obtain a reduced-model approximation we view the large-scale graph as a structured representations with dense areas (clusters) and sparse interconnections between these areas.<sup>CK85</sup>

The network connections  $k_{ij}$  are defined as

$$k_{ij} = \begin{cases} 1, & \text{if the link exists between two nodes} \\ 0 & \text{if no link} \end{cases} \quad (3)$$

We assume having a connectivity network of  $N$  nodes and  $M$  total links yielding thus a  $N \times M$  incidence matrix  $K$  describing this network. The above formulated objectives are achieved by the following network architecture

$$\dot{x}_i = - \sum_{k=1}^M k_{ik} \theta_k, \quad i = 1, \dots, N \quad (4)$$

where  $\theta_k$  represents the difference variable

$$\theta_k := \sum_{l=1}^N k_{lk} x_l = \begin{cases} x_m - x_n & : \text{ if } m \text{ is the positive end,} \\ x_n - x_m & : \text{ if } n \text{ is the positive end} \end{cases} \quad (5)$$

We assume that we have a  $N$ -node network with  $r$  internally dense regions but sparsely connected. Each area has  $m_\alpha$  neurons with  $\alpha = 1, 2, \dots, r$  and the vector  $x^\alpha = [x_1^\alpha \dots x_{m_\alpha}^\alpha]$  contains all neural activities in the area  $\alpha$ . Then we define the slow variable<sup>CK85, BA08</sup> representing an aggregate region as

$$y_\alpha := \sum_{i=1}^{m_\alpha} \frac{x_i^\alpha}{m_\alpha} = \frac{1}{m_\alpha} u_\alpha^T x^\alpha \quad (6)$$

and in matrix representation, we obtain

$$y = M_a^{-1} U^T x \quad (7)$$

with  $M_a = \text{diag}(m_1, m_2, \dots, m_r)$  and  $U = \text{diag}(u_1, u_2, \dots, u_r)$  where each  $u_i$  is an  $m_\alpha$ -vector of 1's.

The fast variable  $z_\alpha$  is given as the transformation of the differences between the activation of the neurons in the same region<sup>CK85, BA08</sup>

$$z_\alpha = Q_\alpha x^\alpha \quad (8)$$

and in matrix formulation we have the fast  $z$  ( $N - r$ )-vector with  $z = [z_1^T z_2^T \dots z_r^T]$

$$z = Qx \quad (9)$$

with  $Q = \text{diag}(Q_1, Q_2, \dots, Q_r)$  being an  $(N - r) \times N$  block diagonal matrix.

We have thus defined a new transformation of the original neural activation  $X$  into a slow and fast variable<sup>BA08</sup>

$$\begin{pmatrix} y \\ z \end{pmatrix} = \begin{pmatrix} M_a^{-1} U^T \\ Q \end{pmatrix} x \quad (10)$$

We assume  $K = K^I + K^E$  with  $K^E$  being the external and  $K^I$  being the internal connection matrix.

The linear singular perturbed system is given as

$$\begin{pmatrix} \dot{y} \\ \dot{z} \end{pmatrix} = \begin{pmatrix} CK^E U & CK^E Q^T \cdot (QQ^T)^{-1} \\ QK^E U & Q(K^I + K^E)Q^T \cdot (QQ^T)^{-1} \end{pmatrix} \cdot \begin{pmatrix} y \\ z \end{pmatrix} \quad (11)$$

where

$$\begin{pmatrix} CK^E U & CK^E Q^T \cdot (QQ^T)^{-1} \\ QK^E U & Q(K^I + K^E)Q^T \cdot (QQ^T)^{-1} \end{pmatrix} = \begin{pmatrix} \tilde{A}_{11} & \tilde{A}_{12} \\ \tilde{A}_{21} & \tilde{A}_{22} \end{pmatrix} \quad (12)$$

We can determine the time-scale model by defining the fast and slow time-scales

$$t_f = c^I t \quad \text{and} \quad t_s = \delta t_f \quad (13)$$

and rescaling the matrices  $A_{ii}$  as

$$\begin{aligned} A_{11} &= \frac{\tilde{A}_{11}}{c^I \delta} & A_{12} &= \frac{\tilde{A}_{12}}{c^I \delta} \\ A_{21} &= \frac{\tilde{A}_{21}}{c^I d} & A_{22} &= \frac{\tilde{A}_{22}}{c^I} \end{aligned} \quad (14)$$

leading to a new system

$$\begin{aligned} \frac{dy}{dt_s} &= A_{11}y + A_{12}z \\ \frac{\delta dz}{dt_s} &= dA_{21}y + A_{22}z \end{aligned} \quad (15)$$

The above model (15) applies to large-scale brain networks for sufficiently small network parameters  $\delta$  and  $d$ . The theoretical results from<sup>CK85</sup> state that the neurons in the same region synchronize in fast time-scale, leading to a substitute aggregate neuron in the slow time-scale.

The above results are summarized in the theorem proven in.<sup>CK85</sup>

**THEOREM 2.1.**<sup>CK85</sup> *There are  $\delta^*$  and  $d^*$  such that for all  $0 < \delta \leq \delta^*$ ,  $0 < d \leq d^*$  the system in equation (15) has  $r$  slow eigenvalues and  $n - r$  fast eigenvalues. The fast and slow subsystems are given as*

$$\begin{aligned} \frac{dy_s}{dt_s} &= (A_{11} - dA_{12}A_{22}^{-1}A_{21})y_s = A_0y_s, \quad y_s(0) = y(0) \\ \frac{dz_f}{dt_f} &= A_{22}z_f, \quad z_f(0) = z(0) + dA_{22}^{-1}A_{21}y(0). \end{aligned} \quad (16)$$

In<sup>CK85</sup> was mentioned a simplified formulation of the slow system, the so-called aggregate system given as

$$M_a \frac{dy_s}{dt} = K_a y_s \quad (17)$$

with  $K_a = U^T K_E U$ .

### 3. PEARSON CORRELATION AND PARTIAL CORRELATION NETWORKS

The standard measure of pairwise correlations are Pearson product-moment correlation coefficients  $P = (\rho_{ij})$ , which quantify the linear dependency between two variables  $l_i$  and  $l_j$ . Pearson correlation networks have been widely applied in imaging connectomics<sup>FZPB12, WRT<sup>+</sup>12</sup> and in addiction research.<sup>YZQ<sup>+</sup>11, SEF<sup>+</sup>16, LYR<sup>+</sup>12, TNM<sup>+</sup>11</sup> A common problem of Pearson correlation coefficients are indirect effects giving rise to a plethora of unspecifically high correlation coefficients. Partial correlation networks attempt to estimate conditional dependencies between measured variables over all samples rather than marginal dependencies, thereby eliminating such indirect correlations. To generate such a network, the number of samples with respect to the number of variables determine the approach used for the calculation. If the number of samples  $n$  exceeds the number of variables  $p$ , full-order partial correlations  $Z = (\zeta_{ij})$  can be calculated in a straight-forward manner from the inverse of the covariance matrix  $P$  as  $\Omega = (\omega_{ij}) = P^{-1}$  and  $Z = (\zeta_{ij}) = -\omega_{ij} / \sqrt{\omega_{ii}\omega_{jj}}$ . A PC graph is an undirected graph obtained by partial correlation calculation with subsequent statistical testing for edge significance. The graph nodes represent the measured variables whereas the edge weights correspond to significant partial correlation coefficients found in the biochemical experiment. In,<sup>WJM<sup>+</sup>12</sup> a novel and more robust algorithm, the PC\* is described, a graph

pruning algorithm for identification of the partial correlation network. A comparison is performed in terms of graph topology in comparison to a network stemming from the direct calculation of partial correlations from the inverse of the sample correlation matrix. The latter one is called the concentration graph.

#### 4. RESULTS OF THE DYNAMICAL GRAPH ANALYSIS OF THE CONCENTRATION AND PC\* CONNECTIVITY NETWORK OF CORTICAL THICKNESS

We apply the theoretical results on structural concentration and PC\* connectivity graphs<sup>WJM+12</sup> for the lateral views of the left and right hemispheres. For the connectivity networks, the cortical gray matter thickness derived from 645 automatically parcellated cortical volumes is analyzed. The covariation in cortical thickness in ROIs defined on a parcellated cortex is represented in such graphs either as a simple concentration or as a PC\*. The nodes in the graphs represent the ROIs while the links show if a connection is existing between these regions or not.

Figure 1 shows the clusters found on the functional data for the lateral view of the left and right hemispheres. We perform a time-scale modeling and area aggregation with two main areas on the four functional networks from Figure 1. For three graphs we can apply Theorem 1, however for the concentration graph, lateral view of left hemisphere, we are not able to obtain an area aggregation since the conditions in Theorem 1 are not satisfied.

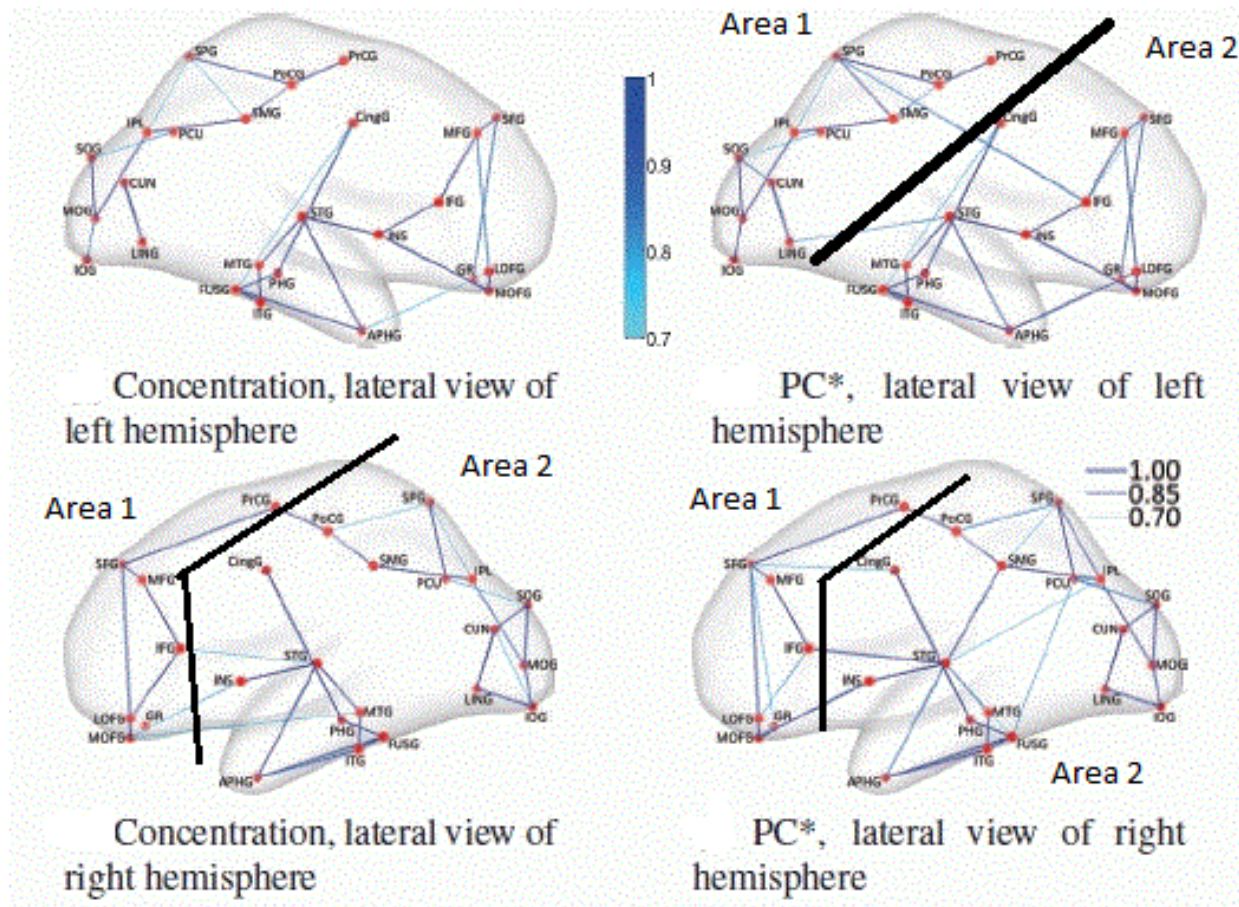


Figure 1. Areas of the connectivity graph for the concentration and PC\* graphs for the left and right hemispheres. Figure adapted from.<sup>WJM+12</sup>

The results of the in-depth dynamical analysis are shown in Table 1. The PC\* show smaller node and area parameters than the concentration graphs. But most importantly, both the exact, as well as the rigid aggregate model as shown in equation (17) show the same eigenvalues for both graphs of the right hemispheres.

Correlation	Node Parameter $d$	Area Parameter $\delta$	Slow $\lambda$ exact system	Slow $\lambda$ rigid aggregate system
Pearson Corr. left	$d_{ave} = 0$	$\delta = 0$	N/A	N/A
PC left	$d_{ave} = \frac{1}{6}$	$\delta = \frac{1}{12}$	$\lambda_i = \{0, -4\}$	$\lambda_i = \{0, -25/77\}$
Pearson Corr. right	$d_{ave} = \frac{4}{7}$	$\delta = \frac{2}{7}$	$\lambda_i = \{0, -8\}$	$\lambda_i = \{0, -50/63\}$
PC right	$d_{ave} = \frac{1}{2}$	$\delta = \frac{1}{4}$	$\lambda_i = \{0, -8\}$	$\lambda_i = \{0, -50/63\}$

Table 1. Area aggregation parameters and time-scale modeling for correlation graphs from Figure 1. The graphs are for the left and right hemisphere.

While the results obtained through PC\* show a better aggregated structure than the concentration graph in terms of node and area parameter, the dynamic graph analysis reveals no different slow modes between concentration and PC\*. The eigenvalues in the right hemisphere are larger than those in the left hemisphere. The contribution of the larger eigenvalues over time decreases quickly. The range of the eigenvalues for each subject represents an important biomarker for disease prediction. By providing an area and node parameter, we are able to add additional static graph descriptors to the dynamic biomarkers.

## 5. DISCUSSION

We applied the new concept of time-scale modeling for sparse networks on graph networks of the cortical thickness between ROIs based on two different PC concepts: the standard concentration matrix concept and a more robust PC\* concept. Our results confirmed the more aggregated structure obtained through the PC\* graph network compared to the standard one, however showed that in terms of dynamics both graphs yield the same dynamical behavior or disease trajectory. It's important to point out that the left hemisphere has a faster dynamics than the right hemisphere meaning that more changes are expected there. While static graph theory shows the changes in graph measures at certain points in time and the differences between disease and normal control, the derived results may have important implication for understanding and controlling the evolution of dementia that may further lead to better therapeutic interventions. Thus by describing the dynamic of the aggregate areas and the resulting time-scale modeling in a brain network, a new research initiative is taken that allows to study in more detail the differences in terms of morphometry between disease and healthy groups and provides a wider variety of characteristic parameters over time for those groups.

## 6. ACKNOWLEDGMENTS

We acknowledge funding through a Fulbright Award.

## REFERENCES

- [BA08] E. Biyik und M. Arcak. Area aggregation and time-scale modeling for sparse nonlinear networks. *Systems and Control Letters*, 57:142–149, March 2008.
- [CK85] J. H. Chow und P. Kokotovic. Time scale modeling of sparse dynamic networks. *IEEE Transaction on Automatic Control*, 30:714–722, 3 1985.
- [FZPB12] A. Fornito, A. Zalesky, C. Pantelis und E. Bullmore. Schizophrenia, neuroimaging and connectomics. *Neuroimage*, 62:2296–2314, 1 2012.
- [GT12] C. Giessing und C. Thiel. Pro-cognitive drug effects modulate functional brain network organization. *Frontiers in Behavioral Neuroscience*, 6:1–9, 1 2012.
- [LMG02] S. Lall, J. Marsden und S. Glavaski. A subspace approach to balanced truncation for model reduction of nonlinear control systems. *Int. Journal of Robust and Nonlinear Control*, February 2002.
- [LYR<sup>+</sup>12] D. Liu, C. Yan, J. Ren, L. Yao, V. Kiviniemi und Y. Zang. Using coherence to measure regional homogeneity of resting-state fmri signal. *Frontiers in Systems Neuroscience*, 6:1–9, 1 2012.
- [MB08] A. Meyer-Bäse. Gene regulatory networks simplified by nonlinear balanced truncation. *SPIE Proceedings Series*, 6979:69790C, 4 2008.
- [MBKEG09] A. Meyer-Baese, A. Koshkouei, M. Emmett und D. Goodall. Global stability analysis and robust design of multi-time-scale biological networks under parametric uncertainties. *Neural Networks*, 22:658–663, 7 2009.
- [MBRT10] A. Meyer-Baese, R. Roberts und V. Thummmler. Local uniform stability of competitive neural networks with different time-scales under vanishing perturbations. *Neurocomputing*, 73:770–775, 4 2010.
- [MBRY07] A. Meyer-Baese, R. Roberts und H. Yu. Robust stability analysis of competitive neural networks with different time-scales under perturbations. *Neurocomputing*, 71:417–420, 11 2007.
- [MBT08a] A. Meyer-Baese und F. Theis. Gene regulatory networks simplified by nonlinear balanced truncation. *SPIE Symposium Computational Intelligence*, 6979:6979C, 7 2008.
- [MBT08b] A. Meyer-Baese und V. Thummmler. Local and global stability analysis of an unsupervised competitive neural network. *IEEE Transactions on Neural Networks*, 19:346–351, 5 2008.
- [MBTC11] A. Meyer-Bäse, F. Theis und C. Conrad. Uncertain gene regulatory networks simplified by gramian-based approach. *International Conference on Bioinformatics and Computational Biology 2011*, Seite In print, 4 2011.
- [Moo81] B. Moore. Principal component analysis in linear systems: controllability, observability and model reduction. *IEEE Transactions on Automatic Control*, Seiten 17–32, January 1981.
- [Sch93] J. Scherpen. Balancing for nonlinear systems. *Systems and Control Letters*, Seiten 143–153, March 1993.
- [SEF<sup>+</sup>16] A. Smith, A. Ehtemami, D. Fratte, A. Meyer-Baese, O. Zavala-Romero, A. Goudriaan, L. Schmaal und M. Schulte. Functional connectivity analysis of resting-state fmri networks in nicotine dependent patients. *Medical Imaging 2016: Biomedical Applications in Molecular, Structural, and Functional Imaging*, 9788:978827, 1 2016.
- [SK84] Ali Saberi und Hassan Khalil. Quadratic-type lyapunov functions for singularly perturbed systems. *IEEE Transactions on Automatic Control*, Seiten 542–550, June 1984.
- [TNM<sup>+</sup>11] J. Tanabe, E. Nyberg, L. Martin, D. Cordes, E. Kronberg und J. Tregallas. Nicotine effects on default mode network during resting state. *Psychopharmacology*, 216:287–295, 4 2011.
- [WJM<sup>+</sup>12] D. Wheland, A. Joshi, K. McMahon, N. Hansell, N. Martin, M. Wright, P. Thomson, D. Shattuk und R. Leahy. Robust identification of partial-correlation based networks with applications to cortical thickness data. *9th IEEE International Symposium on Biomedical Imaging (ISBI)*, 3:1551–1554, 5 2012.
- [WRT<sup>+</sup>12] K. Wylie, D. Rojas, J. Tanabe, L. Martin und J. Tregallas. Nicotine increases brain functional network efficiency. *Neuroimage*, 63:73–80, 1 2012.



- [YZQ<sup>+</sup>11] R. Yu, L. Zhao, W. Qin, W. Wang, K. Yuan, Q. Li und L. Lu. Regional homogeneity changes in heavy male smokers: a resting-state functional magnetic resonance imaging study. *Addiction Biology*, Seiten j.1369–1600, 4 2011.
- [ZSL<sup>+</sup>12] L. Zeng, H. Shen, L. Liu, L. Wang, B. Li, P. Fang, Z. Zhou, Y. Li und D. Hu. Identifying major depression using whole-brain functional connectivity: a multivariate pattern analysis. *Brain*, 1498:1498–1507, 4 2012.